

The Tribocharging Behavior in Toner–Carrier Systems

Ching-Yu Chou and Arnold C.-M. Yang

Department of Materials Science and Engineering, National Tsing-Hua University, Hsinchu, Taiwan

The tribocharging behavior of toners in the toner/carrier system dictates the final output results of the electrophotographic system. However, the available theoretical models describe only the charging results in the equilibrium state and leave the charging during the transient state almost untouched. Therefore, in this paper the charging behavior of a toner–carrier development system were carefully examined and a dynamic model that could account for the charging process of both the transient and equilibrium states was constructed. The influences on charging due to the physical parameters of charging time, toner sizes, and toner concentration were studied by measuring the charge-to-mass ratio (Q_t/M_t). The relationship between charges and charging surface was also studied. The predicted dynamic results from the model are in good agreement with the observed data.

Journal of Imaging Science and Technology 46: 208–215 (2002)

Introduction

Tribocharging behavior of toners is very important in electrophotography and it has a determinant influence on the final output. However, the details of the charging process are still unclear. Charging is generally believed due to exchange of charge entities between contact surfaces, but it is still unclear whether the charged entities are either electrons, ions, or perhaps both. For example, although some experiments^{1–4} have shown that ion concentration and polymer side group species of the contact surfaces could be related to charging, other experiments⁵ still cannot be fully explained by the ion transfer theory. To date, the only theories that can quantitatively account for the charging behavior are the surface state theories based on electron transfer. The earliest of these was first proposed by Lee⁶ in 1978 who considered tribocharging to be a charge transfer phenomenon driven by the difference in the Fermi levels of the contact surfaces. During the tribo-contacts, electrons transfer between surfaces until the two Fermi levels equal. Based on this criterion equality, the toner charging of a toner–carrier system can be described as follows,

$$\frac{M_t}{Q_t} = r_c \frac{M_t}{M_c} \frac{\rho_c}{3e f_c N_c \Delta\phi} + r_t \frac{\rho_t}{3e f_t N_t \Delta\phi} \quad (1)$$

where Q_t is the charges generated on toner, M_t is the mass of toner, f is the effective surface area ratio of toner to carrier, the symbols of M , r , N , $\Delta\phi$, and ρ represent respectively the mass, radius, surface state density, the Fermi level difference, the effective surface area ratio, and charge density; and subscript t and c refer to two

contact surfaces of toner and carrier respectively. A linear relationship between mass-to-charge ratio of toners (M_t/Q_t) and the mass ratio of toners and carriers (M_t/M_c) was predicted by Eq. 1 and was subsequently verified by experiments.^{6–8} Lee's model basically is an extension of the conductor charging system of metal–metal contacts to the cases of insulator charging of the toner–carrier systems.

In 1992, Schein⁹ proposed a new model. Instead of emphasizing the equilibrium of Fermi levels, a force balance between local state was taken into consideration. On his assumption, the charge transfer was accomplished with an electric field balance between one due to the local electron transfer and that from the work function difference. The toner charging behavior in comparison to Lee's model is

$$\frac{M_t}{Q_t} = r_c \frac{M_t}{M_c} \frac{\rho_c}{3\epsilon_0 E_e} + r_t \frac{\rho_t}{3\epsilon_0 E_e} \quad \text{where } E_e = \frac{\Delta\phi}{ez} \quad (2)$$

where z represents the charge transfer cease distance, i.e., the distance beyond which charge transfer never takes place. The linear relationship described in Eq. 1 was also demonstrated here in Eq. 2. However, Eq. 2 showed that slope-to-intercept ratio in the plot of M_t/Q_t versus M_t/M_c was dependent only on the radius and densities of the toners and carriers particles, which could not be explained by the model presented by Lee.^{9,10}

In 1994, Anderson¹¹ asserted that charging equilibrium was achieved by the influence of the both factors of local electric field effect and work function difference. The toner charging result becomes

$$\frac{M_t}{Q_t} = -\frac{z}{3\epsilon_0(\Delta\phi)} \left[\frac{\epsilon_0 r_t \rho_t}{N_t e z} + \frac{M_t}{M_c} \frac{\epsilon_0 r_t \rho_t}{N_t e z} + e r_t \rho_t + \frac{M_t}{M_c} e r_c \rho_c \right] \quad (3)$$

Original manuscript received September 18, 2000

©2002, IS&T—The Society for Imaging Science and Technology

It is interesting that Eq. 3 reduces to Eq. 2 when

$$\frac{\varepsilon_0}{N_t e^2 z} \ll 1 \text{ and } \frac{\varepsilon_0}{N_c e^2 z} \ll 1,$$

i.e., a situation corresponds to the high density extreme of localized states. On the other side, when in low density states extreme, that is

$$\frac{\varepsilon_0}{N_t e^2 z} \gg 1 \text{ and } \frac{\varepsilon_0}{N_c e^2 z} \gg 1,$$

Eq. 3 converts into Lee's results of Eq. 1. However, the parameters in the equation are so many that it is difficult to verify experimentally. Nevertheless, all three models described above only explain the equilibrium state of tribocharging.

The purpose of this study is first to explore the tribocharging behavior of a toner-carrier system via examination of the effects of the fundamental physical parameters of tribocharging time, particle sizes, and surface area ratio of the two charging surfaces.¹² Then a simple statistical charging model was constructed to describe the process of contact charging between the two type of particle surfaces.¹³ The phenomena of both the transient and equilibrium states of tribocharging can therefore be revealed.

Experimental Procedures

Materials

Canon SX-compatible toner without extraparticulates that was formulated, made, and kindly supplied by Trend Tone Imaging Technology was exclusively used throughout this experiment. The toner particles were approximately 13 μm in diameter with a true density of 1.5 g/cm^3 and an apparent density of 0.53 g/cm^3 . The carrier particles bought from Powder Tech (F141-1030) used were copper nickel ferrite ($(\text{Cu}_x\text{Ni}_{1-x})\text{O} \cdot \text{Fe}_2\text{O}_3$) cores coated with acrylic resins. They were 82 μm in diameter with a true density of 5.5 g/cm^3 truly and an apparent density of 2.6 g/cm^3 .

Equipment

A Q/M meter was used to measure the charge-to-mass ratio (Q_t/M_t) of toners by the blow-off method. It was composed of an air pump, a Faraday cage with fine mesh filters at both ends, and an electrometer. When toner and carrier were finished mixing, the generated tribocharging was determined by placing a few grams of the toner-carrier mixture in the Faraday cage. An air flow was blew through the cage, separating the small toner particles from the large carrier particles by filtration of the fine meshes. The separation process produced net charges in the cage, which could be measured with the electrometer to obtain the toner charge Q_t/M_t . The distribution of toner charge versus particle size can be determined by use of a Q/D meter. The operational principle utilizes the force equilibrium between electric forces and the Stokes drag forces on toner particles. Detailed descriptions of the operations and equipment were referred to previous publications by Williams and the references therein.¹⁴⁻¹⁶ The Q/M and Q/D meters were made by Epping GMBH.

Charging Experiments

For the toner charging experiment, the toner and carrier particles were mixed in a plastic bottle of polyethyl-

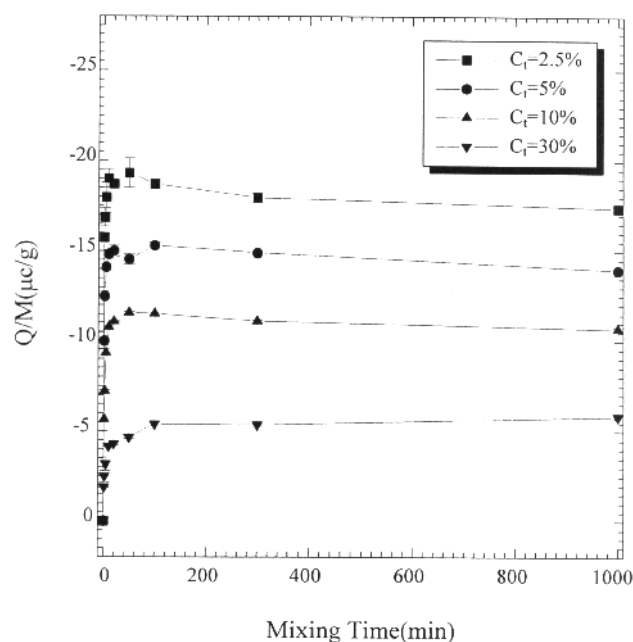


Figure 1. The relationship between toner charge Q_t/M_t and mixing time during charging.

ene in a roller mixer with a speed of 200 rpm for 1 min. The toner concentration in the mixture C_t is defined as the toner weight/total weight of the mix. After mixing, a few grams of the charged mixture was picked to test the toner charge-to-mass ratio Q_t/M_t in Q/M meter. Usually, five measurements of the charged mixture were carried out to obtain the average Q_t/M_t value. The same procedure was repeated for a variety of mixing times of 2, 5, 10, 20, 50, 100, 300, 1000 minutes so that the influence of charging time on charging could be investigated. The effect of toner concentration C_t was also investigated. The C_t values were 2.5%, 5%, 10%, and 30%.

Experimental Results

Charge versus Mixing Time

The relationship between the toner charges Q_t/M_t and mixing time was shown in Fig. 1, where the four curves indicated different toner concentrations ($C_t = 2.5\%, 5\%, 10\%, 30\%$). For all toner concentrations, Q_t/M_t increased gradually with a decreasing rate to a final plateau value as mixing time increased in all concentrations. The time for the toner charges to saturate to a constant value is called the saturation time τ .

Charge versus Toner Concentration

The relationship between Q_t/M_t and C_t was shown in Fig. 2, where the nine curves indicated different charging times: $t = 1, 2, 5, 10, 20, 50, 100, 300$, and 1000 minutes. From the curves, Q_t/M_t always decreased gradually with decreasing rate as toner concentration increased. The charging rate, however, was found to vary with toner concentrations. As shown in Fig. 3, the time to the saturation charge τ was found to be longer with greater C_t . The relationship between τ and C_t was shown in Fig. 4.

Charge versus Toner Size

The positive relationship between toner charges and the particle size was shown in Fig. 5 for different toner diameters $d = 3.2, 5.4, 7.3, 9.2, 11.1, 13.2, 15.1, 17.1$ μm . For greater toner particles, the toner charge Q_t/M_t

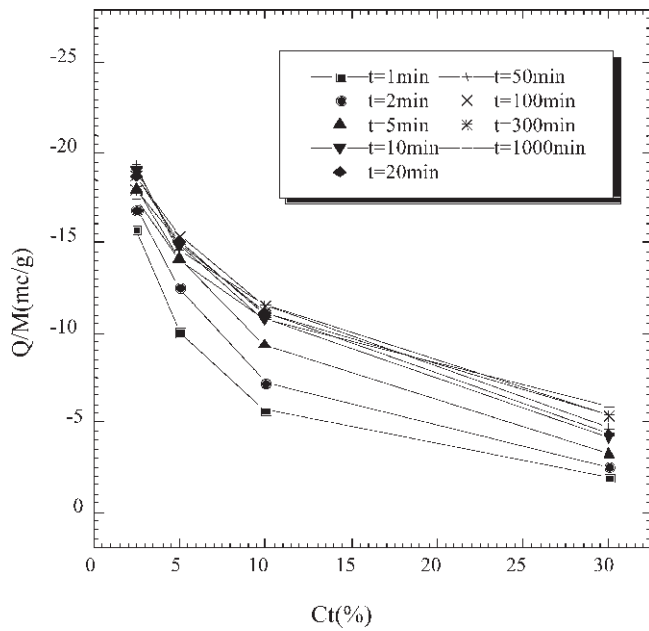


Figure 2. The relationship between toner charge Q_t/M_t and toner concentration C_t .

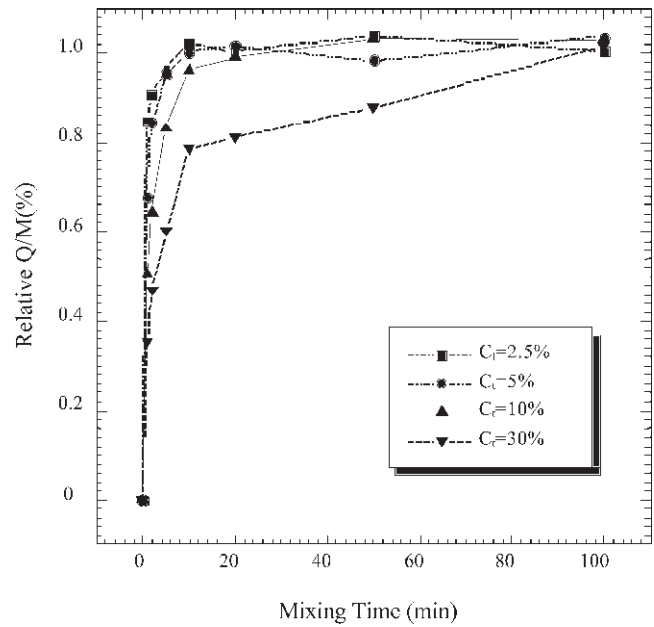


Figure 3. The relationship between relative toner charge Q_t/M_t and mixing time during charging.

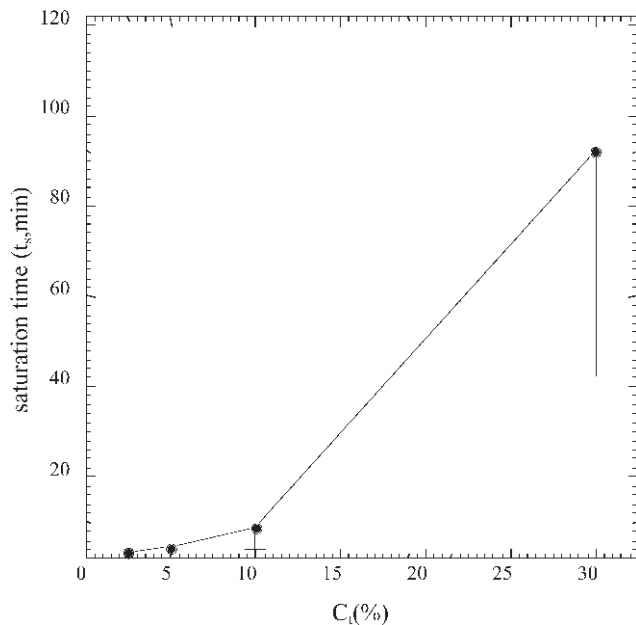


Figure 4. The relationship between charge saturation time τ and toner concentration C_t .

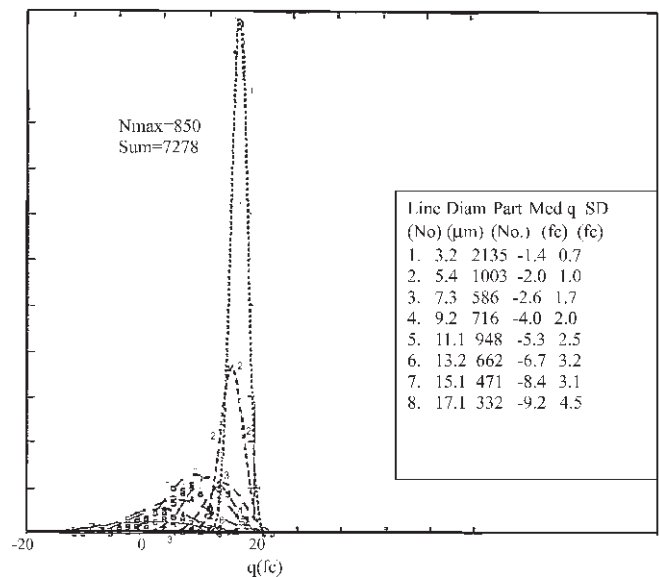


Figure 5. The relationship between toner charge distribution and toner particle size.

was found to increase and the charge distributions of Q_t/D_t became broader. In a further examination as shown in Fig. 6, the toner charge increases with the square of toner particle radius, but with a small positive intercept of charge for $Q_t = 0$.

Discussions

Effect of Mixing Time

The physical meaning of 'mixing' in tribocharging should be considered in order to understand the relationship between Q_t/M_t and mixing time. 'Mixing' provides

the chance for toners and carriers to contact, i.e., the chance to transfer the charged entities. Therefore, as the mixing time becomes longer, more contacts take place, hence the transferred charge and the measured Q_t/M_t value increase. However, due to the expulsion effect of electrostatic charges, the charge transfer will become more difficult once charge transfer already takes place. Alternately, in the view of surface state models, once charge transfers, the work function difference decreases, so as the driving force for charge transfer. Therefore, the toner charging curve finally flattened out to a plateau value as seen in Fig. 1.

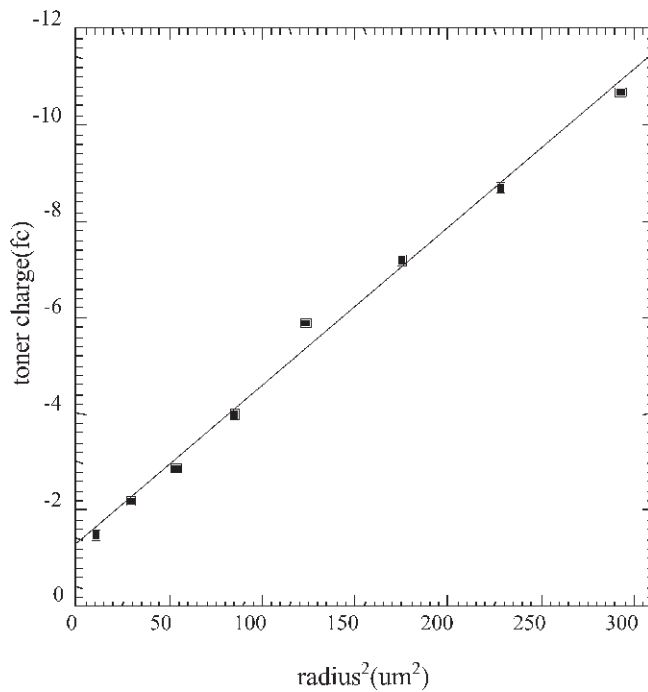


Figure 6. The relationship between toner charge Q per particle and the square of toner radius r^2 . The toner charge is determined from the median value of the charge distribution. The data indicate a relationship between Q and r to be $Q = -1.3 - 0.33r^2$.

Effect of Toner Concentration

As toner concentration increases, the fraction of carriers decreases, and the charges provided to toner also decrease. Meanwhile, as the number of toners increases, the charges shared per toner particle decreases. Therefore, the Q_t/M_t decreased when C_t increased.

Effect of Toner Size

Because tribocharging surface reactions are closely related to the number of available states on the surface, larger toner particles would be able to undergo more charge transfer compared to smaller ones. Hence, the toner charges increase linearly with the surface area of the toner particles, as indicated in Figs. 5 and 6. Also, if there exists a minimum charge transfer per contact, the smaller toner particles should have narrow charge distributions compared to the larger particles. This assertion will be further discussed in the next section by the calculation of charge transfer per toner-carrier contact. However, the small positive intercept of charge in Fig. 6 is puzzling from the point of view of the work function mechanism. It seems to suggest that there is another mechanism existing besides what had discussed in the previous sections. The positive charge intercept seems to indicate the effect of friction on charge transfer during the tribocharging process. Charge transfer induced by friction was observed and was discussed previously by Harper¹⁷ and Lowell.¹⁸ Also, fracture induced charge particle emission in various materials including polymers was well documented by Dickinson.^{19–21} Therefore, the positive charge intercept is attributed to the effect of friction or surface micro-fracture. The effect, however, is small compared to that due to work function charge transfer.

Charge Transfer Per Contact

How many electrons “jump” over during a toner-carrier contact? In an attempt to explore the answer of the above question, the mean free path of an average toner particle during tribocharging was estimated. All toners and carriers are assumed to be spherical and the radius of toner and carrier are r_t and r_c respectively. During tribocharging, if the center-to-center distance between a toner and a carrier is equal to the sum of the two radius ($r_t + r_c$), these particles will make a contact. It is also assumed that during tribocharging in each turn of the charging bottle of 4 cm diameter, an average toner particle travels 2 cm. Hence, a tube with a diameter of ($r_t + r_c$) swept by the trajectory of the toner particle is the “contact zone” in which the toner particle will make a contact with a carrier if a carrier happens to be in the tube. The volume of the tube v_{tube} is

$$v_{tube} = \pi(r_t + r_c)^2 \cdot 2 = 1.4 \times 10^{-4} \text{ cm}^3 \quad (4)$$

in which the probability that the toner particle meets a carrier is equal to the volume fraction of carrier ($1 - C_t$) of the mixture. Therefore, the number of toner-carrier contacts, N , for that toner particle during one revolution is

$$N = (v_{tube}/v_t) (1 - C_t) \quad (5)$$

where v_t is the volume of a toner particle. Substitute all the system parameters into calculation ($C_t = 5\%$; true density of toner and carrier = 1.5 g/cm³ and 5.5 g/cm³; apparent density of carrier = 2.6 g/cm³), we have $N = 217$ per revolution per toner particle. For a rotation velocity of the charging bottle to be 200 rpm, a toner particle will contact 4.3×10^4 times with carriers. From 1 minute charging, the toner charging $Q_t/M_t = -10 \mu\text{Coul/g}$, hence 3.3 electrons were transferred per contact.

Comparison with the Existing Equilibrium Models

The relationship between the reciprocal of toner charge M_t/Q_t and the mass ratio (M_t/M_c) is shown in Fig. 7. It is a straight line just as the models of low surface state density (Eq. 1) and high surface state density (Eq. 2) had predicted. First take the high surface state extreme to be correct, the local electric field could be calculated from straight line in Fig. 9 according to Eq. 2 either from the intercept or the slope. Two very different electric field values were obtained: 2.634×10^8 (C/cm-F) (from the intercept) and 8.07×10^6 (C/cm-F) (from the slope), which should be identical, however. Secondly, try the low surface density extreme, and treat the two surfaces of contact (toner and carrier) to be a parallel capacitance C . In this case, the charge transfer cease distance z and the work function difference $\Delta\phi$ are related as

$$\Delta\phi = \frac{q^2}{2C} = \frac{q^2 z}{2A\epsilon_0} \quad (6)$$

where q is the transferred charge per contact and A is the area of the parallel plate. Because the transfer charges are estimated to be 3.3 electrons per contact, the cease distance is calculated from Eq. 6 to be 5.4 nm. Although the tunneling stop at 1 nm, however, due to the local roughness of toner powder being the order of several nm, the result seems reasonable. Based on these comparisons, our experiment seems to be better

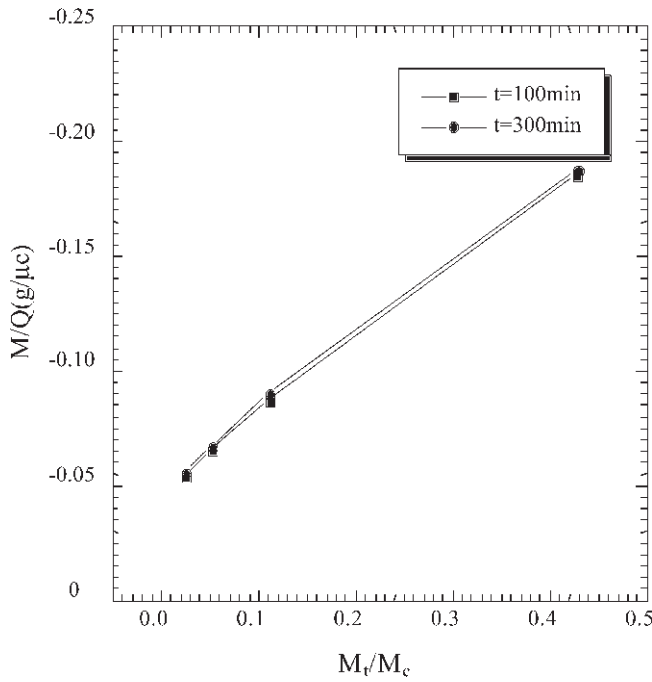


Figure 7. The relationship between M_t/Q_t and mass ratio (M_t/M_c).

fit with the low surface density model satisfying the conditions of

$$N_t \ll \frac{\epsilon_0}{e^2 z} \text{ and } N_c \ll \frac{\epsilon_0}{e^2 z}$$

in Anderson's formula. The surface concentration and dispersion of the charge control agents in the toner formulation seems to have important effect on the surface state density of toner particles.

A Dynamic Tribocharging Model

As stated previously, the existed models of charge transfer were derived in the view of equilibrium energy states, hence they could not describe or explain what happen in the transient states. The tribocharging processes usually take a long time to reach equilibrium. For instance, the toner used in this study requires at least 5 minutes to reach equilibrium, as shown in Fig. 1. Further, the transient state charge transfer information is critical for material formulation for toners, carriers, and flow agent, as well as machine design. Henceforth, the dynamic charging process of toner and carrier particles is very important. For simplicity, the charging system composed of only toner and carrier particles was considered.

The dynamic charging process was modeled using a statistical approach by first considering the charging process of an average toner particle. To calculate the accumulated charges that a toner particle can obtain after a fixed time of tribocharging, the major charge transfer mechanism of toner-carrier surface interactions was considered only, and the other minor mechanisms, e.g., the toner-toner or carrier-carrier surface interactions, were ignored. For the purpose of calculation, the charging process was artificially divided into many short consecutive time periods in each a toner particle has a finite possibility ψ of making contact with a carrier particle. The time periods were small such that

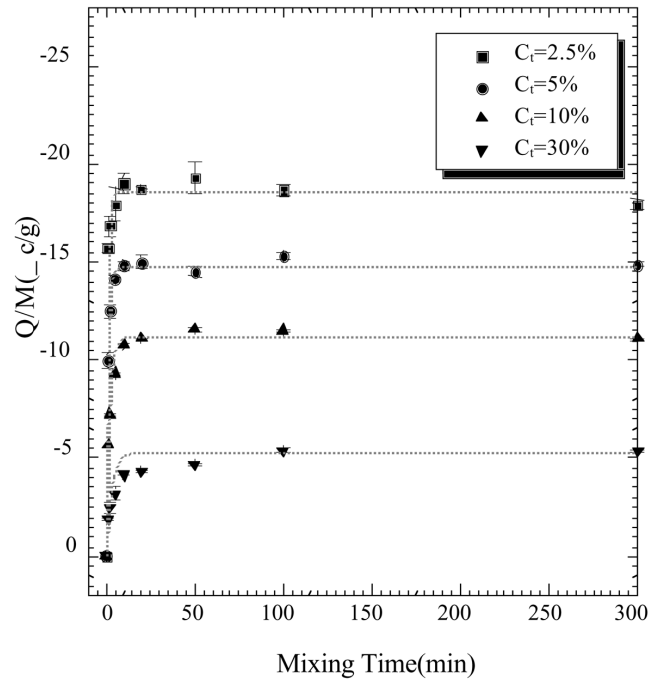


Figure 8. The comparison of charge experimental results and the calculation from the dynamic charging model.

$\psi \leq 1$. The contact possibility ψ between toners and carriers during tribocharging is assumed to be constant with time and depends only on the system parameters, e.g., C_c . Further, charge transfer between toners and carriers is determined only by their surface properties which are assumed to be homogeneous. The toner particle surface was then artificially divided into many small local regions that can undergo independent charge transfer. Same assumption was also made for carrier particles. Each local surface region on toner particles would instantly reach the work function equilibrium with the local region of a carrier that it contact, but once charges q were transferred the local toner region would not participate further in the charging process. Similarly, the local regions on carrier particles were assumed to follow the same charging behavior as their toner counterparts. According to previous analysis, the charge transfer q per contact is 3.3 electrons.

For the purpose of clarity, the following variables was used:

- ψ : the contact possibility between toners and carriers in each time period,
- $P_{t,i}$: the probability of charge transfer to toner during contacts in time period i ,
- $P_{c,i}$: the probability of charge transfer to carrier during contacts in time period i ,
- A_t : total surface area of a toner particle,
- A_c : total surface area of a carrier particle,
- a_t : surface area of the local contact region of a toner,
- a_c : surface area of the local contact region of a carrier,
- α : the number ratio of toner particles to carrier particles.

Consider first the charging of a toner particle. For an arbitrary time period i , the probability of charging of a toner particle, $P_{t,i}$, is the product of possibility of contact with a carrier particle, ψ , and the surface ratios of effective charging area (the uncharged surface area) ξ_t and ξ_c of the toner and carrier particles respectively,

$$P_{t,i} = \psi \xi_t \xi_c \quad (7) \quad \text{the term}$$

Because

$$\xi_t = 1 - \frac{a_t}{A_t} P_{t,i-1}$$

and

$$\xi_c = 1 - \frac{a_c}{A_c} P_{c,i-1},$$

we have

$$P_{t,i} = \psi \left[1 - \frac{a_t}{A_t} P_{t,i-1} \right] \left[1 - \frac{a_c}{A_c} P_{c,i-1} \right] \quad (8)$$

Due to charge neutrality of the whole system, the following relation should hold

$$P_{c,i} = \alpha P_{t,i} \quad (9)$$

where α is defined as the ratio of the number of toner particles/the number of carrier particles

$$\alpha \equiv \frac{\text{number of toner particles}}{\text{number of carrier particles}}$$

$$= \frac{C_t r_c^3 \rho_c}{(1 - C_t) r_t^3 \rho_t} \quad (10)$$

Therefore,

$$P_{t,i} = \psi \left[1 - \frac{a_t}{A_t} P_{t,i-1} \right] \left[1 - \frac{a_c}{A_c} \alpha P_{t,i-1} \right] \quad (11)$$

The charging probability $P_{t,i}$ can be derived further in a simple form as shown in the following calculation. In the time period 1, because there are no previous charging events, we have $\xi_t = 1$ and $\xi_c = 1$, hence

$$P_{t,1} \equiv P_{t,i=1} = \psi \quad (12)$$

From Eq. 5 and Eq. 6, the charging probability in time period 2 is

$$\begin{aligned} P_{t,2} &= \psi \left[1 - \frac{a_t}{A_t} \psi \right] \left[1 - \frac{a_c}{A_c} \alpha \psi \right] \\ &= \psi \left[1 - \frac{a_t}{A_t} \psi - \frac{a_c}{A_c} \alpha \psi + \frac{a_t}{A_t} \frac{a_c}{A_c} \alpha \psi^2 \right] \end{aligned} \quad (13)$$

Because

$$\frac{a_t}{A_t} \frac{a_c}{A_c} \alpha \psi^2 \ll \frac{a_t}{A_t} \psi$$

or

$$\frac{a_c}{A_c} \alpha \psi,$$

is neglected and $P_{t,2}$ becomes

$$P_{t,2} \equiv \psi \left[1 - \frac{a_t}{A_t} \psi - \frac{a_c}{A_c} \alpha \psi \right] \equiv \psi \kappa \quad (14)$$

where

$$\kappa \equiv \left[1 - \frac{a_t}{A_t} \psi - \frac{a_c}{A_c} \alpha \psi \right].$$

Following the same way by using Eqs. 11 through 14, the charging probability of the toner particle in time period 3, $P_{t,3}$, is

$$\begin{aligned} P_{t,3} &= \psi \left[1 - \frac{a_t}{A_t} \psi - \frac{a_t}{A_t} \kappa \psi \right] \left[1 - \frac{a_c}{A_c} \alpha \psi - \frac{a_c}{A_c} \kappa \psi \right] \\ &\equiv \kappa \psi \left[1 - \frac{a_t}{A_t} \psi - \frac{a_c}{A_c} \alpha \psi + (2 + \kappa) \frac{a_t}{A_t} \frac{a_c}{A_c} \alpha \psi^2 \right] \\ &= \kappa \psi^2 \end{aligned} \quad (15)$$

and we have for $P_{t,i}$

$$P_{t,i} = \kappa \psi^{i-1} \quad (16)$$

Therefore at time t the total charges a toner accumulates are

$$Q_t' = \sum_{i=0}^t q P_{t,i} = q \psi \frac{1 - \kappa^t}{1 - \kappa} \quad (17)$$

Henceforth, the total toner charges are Q_t' multiplied by the number of toner particles to be

$$Q_t = \left[q \psi \frac{1 - \kappa^t}{1 - \kappa} \right] \left[\frac{M_t}{\frac{4}{3} \pi r_t^3 \rho_t} \right] = \frac{3q(1 - \kappa^t) M_t}{4\pi r_t^3 \rho_t \left[\frac{a_t}{A_t} + \frac{a_c}{A_c} \alpha \right]} = K(1 - \kappa^t) \quad (18)$$

where

$$K = \frac{3q M_t}{4\pi r_t^3 \rho_t \left[\frac{a_t}{A_t} + \frac{a_c}{A_c} \alpha \right]}.$$

To compare with the results of the low and high surface state density models, Eq.8 can be expressed as

$$\frac{M_t}{Q_t} = \frac{4\pi r_t^3 \rho_t \left(\frac{a_t}{A_t} + \frac{a_c}{A_c} \alpha \right)}{3q(1 - \kappa^t)} \quad (19)$$

Because $\kappa < 1$ when the time t is large, the factor $(1 - \kappa')$ approaches unity, M_t/Q_t becomes time independent, corresponding to the equilibrium charging result. Combining Eq. 19 for large t and Eq. 10 gives the equilibrium state result

$$\frac{M_t}{Q_t} = \frac{r_t \rho_t}{3(\frac{q}{a_t})} + \frac{C_t}{1 - C_t} \frac{r_c \rho_c}{3(\frac{q}{a_c})} = \frac{r_t \rho_t}{3(\frac{q}{a_t})} + \frac{M_t}{M_c} \frac{r_c \rho_c}{3(\frac{q}{a_c})} \quad (20)$$

Comparisons Between the Dynamic Model and Tribocharging Results

Charge versus Mixing Time

The time dependent relationship derived from the dynamic model, Eq. 19, is an exponential saturation curve. It is in good agreement with the charging data of the tribocharging experiments, as shown in Fig. 8.

Consider the length of charging time τ to the equilibrium Q_t/M_t value. From Eq. 19, in order for Q_t/M_t becoming a time-independent value, rigorously κ^{ts} must approach to zero. However, let's consider a τ that leads to the quasi-equilibrium value of Q_t/M_t , i.e., $\kappa^\tau = \zeta$ in which ζ is a very tiny value. Because $\ln \kappa^\tau = \ln \zeta$, we should have

$$\tau = \ln \zeta / \ln \kappa = \ln \zeta / [(a_t/A_t) \Psi + (a_c/A_c) \alpha \Psi] \propto 1/\Psi \quad (21)$$

Therefore, charge saturation time τ is inversely proportional to Ψ . Because Ψ is proportional to the roller speed, so τ is also inversely proportional to the roller speed. It is in excellent agreement with Anderson's experimental result²² that shows that the charge saturation time is inversely proportional to roller speed. Finally, since $\tau \propto 1/\Psi$, the contact probability Ψ decreases due to fewer carrier particles, and result in a longer charge saturation time τ greater toner concentration C_t . This prediction is consistent with our experimental observations shown in Fig. 4.

Charge versus Toner Concentration

The concentration dependence of Q_t/M_t has been derived in Eq. 20, which predicts that for a fixed charging time, Q_t/M_t will be smaller with a larger C_t . This prediction is in good agreement with the experimental results shown in Fig. 2. Furthermore, at the time independent extreme, Eq. 20 has a similar form as those derived in the previous equilibrium models in which the linear relationship of M_t/Q_t and the mass ratio M_t/M_c is well explained. The slope-to-intercept ratio is shown in Eq. 20 to be related in the following to the radii, densities, and local contact areas of the toner particles and carriers:

$$\frac{\text{slope}}{\text{intercept}} = \frac{a_c r_c \rho_c}{a_t r_t \rho_t} \quad (22)$$

Because a_t and a_c should be comparable in size but not necessarily equal, it can be well understood why slope-to-intercept is not exactly equal to the radius and densities ratio between carriers and toners as found in previous publications.^{9,10} The local contact areas a_t and a_c of toner and carrier, can be obtained following Eq. 10 from the slope and intercept of the M_t/Q_t versus M_t/M_c plot. The slope is found to be 0.32 g/ μ Coul and the intercept is 0.049 g/ μ Coul. According to the previous calcu-

lation, the charge transfer per contact q is 3.3 electrons. The local contact area on carrier particles a_c calculated from the slope is $2.3 \times 10^{-11} \text{ cm}^2$, or $(0.05 \mu\text{m})^2$. Likewise, the local contact area on the toner particles a_t calculated from the intercept is $7.4 \times 10^{-11} \text{ cm}^2$, or $(0.09 \mu\text{m})^2$. Both the local contact areas on toner and carrier are much less than the surface area of a single toner or carrier particle. These numbers are reasonable results, further supporting that tribocharging is closely related to the local surface contact of toner and carrier particles.

Comparisons with the Previous Dynamic Model

Gutman and Hartmann^{23,24} recently proposed a comprehensive tribocharging model in which the saturated charging level was theoretically deducted and fit into an empirical equation that describes the exponential saturated time dependence behavior:

$$\frac{q}{m} = \frac{A_0}{C + \Omega_0(C)} [1 - \exp(-\frac{t}{\tau})] \quad (23)$$

In the equation, the factor

$$\frac{A_0}{C + \Omega_0(C)}$$

is the theoretical result deducted from considerations of the electric field of toner-carrier interface in mono-layer or multi-layer toner coverage. The time dependent part of the equation,

$$\left[1 - \exp\left(-\frac{t}{\tau}\right) \right],$$


however, was purely empirical, hence, lack clear explanation. For example, the time constant τ in Eq. 23 was not a fixed constant for each toner concentration and not given a physical meaning. In contrast, the dynamic model presented in the previous section was derived based on the contact probability as well as the charge transfer probability, through which the toner concentration and contact surface properties dictate the time dependence of tribocharging. Furthermore, because the dynamic model presented here is not derived from the electric field between toners and carriers, it can be applied to mono-component systems and, after some modifications, to the special dual-component systems where carrier is conductive. The work is currently being endeavored by the authors.

Conclusions

We have systemically studied the important physical factors which influence the charging behavior of the toner-carrier systems and concluded that:

1. Charging is related to the length of mixing time, in that as time increases the toner charges Q_t/M_t increases gradually with decreasing rate to the final plateau value.
2. Charging is also related to the toner concentration C_t in the toner-carrier system in that Q_t/M_t decreases gradually with decreasing rate as C_t increases. Moreover, the charging rate is slower with larger C_t and the time to saturation charge t is greater for larger C_t values.
3. Charging is related to the size of the toner particles in that larger toners have more charges. The toner

charge per particle increases linearly with the square of toner's radius.

4. A dynamic charging model in a toner-carrier system was derived. It successfully describes both our experimental results and that of previous workers. The equilibrium as well the transient charging behavior can be explained. Because the model was derived without the assumption that electron transfer is the only charging mechanism, it may also apply to cases in which ion transfer or frictional charging is the dominant charge transfer mechanism. The local charging areas of the two contacting surfaces can be calculated using this model. 

Acknowledgements. We would like to thank the friends in Industrial Technology Research Institute (ITRI) in Taiwan, particularly to Ms. Ming-Chu Wu who had provided so much help in the whole program, and to Juei-Tsang Hsu and Han-Chung Wang for their advice during the course of the study, and finally to Yau-Song Yang for conducting the important charging experiments on the machine stand. Finally we would like to express our gratitude to Trend Tone Imaging for kindly supplying the toners used in the experiments.

References

1. D. E. Bugner and J. H. Anderson, *ACS National Meeting: Polymer Reprints 1988*, **29**, 463 (1988).
2. A. Diaz, D. Fenzel-Alexander, D. C. Miller, D. Woolmann and A. Elgenberg, *Proceedings of the 6th Int'l. Congress on Advances in Non-Impact Printing Technologies*, IS&T, Springfield, VA, 1990, 178.
3. C. M. Seymour and A. Diaz, *Proceedings of the 6th Int'l. Congress on Advances in Non-Impact Printing Technologies*, IS&T, Springfield, VA, 1990, p. 184.
4. A. Diaz, D. Fenzel-Alexander and D. Woolmann, *J. Poly. Sci. B: Poly. Phys.* **29**, 1559 (1991).
5. M. Seymour, D. Woolmann, D. Dreblow and A. Diaz, *Proceedings of the 8th Int'l. Congress on Advances in Non-Impact Printing Technologies*, IS&T, Springfield, VA, 1992, p. 119.
6. L. H. Lee, *Photogr. Sci. Eng.* **22**, 228 (1978).
7. J. T. Bickmore and R. J. Nash, *Proceedings of the 8th Int'l. Congress on Advances in Non-Impact Printing Technologies*, IS&T, Springfield, VA, 1992, p. 113.
8. J. H. Anderson, *J. Imaging Sci.*, **33**, 2000 (1989).
9. L. B. Schein, *Proceedings of the 8th Int'l. Congress on Advances in Non-Impact Printing Technologies*, IS&T, Springfield, VA, 1992, 35; *J. Imaging Sci. Technol.*, **37**, 1 (1993).
10. G. S. P. Castle and L. B. Schein, *Proceedings of the 10th Int'l. Congress on Advances in Non-Impact Printing Technologies*, IS&T, Springfield, VA, 1994, p. 114.
11. J. H. Anderson, *J. Imaging Sci. Technol.* 1994, **38**, 378 (1994).
12. A. C.-M. Yang, C.-Y. Chou, J.-T. Hsu, *Proceedings the 11th Int'l. Congress on Advances in Non-Impact Printing Technologies*, IS&T, Springfield, VA, 1995, p. 130.
13. A. C.-M. Yang, C.-Y. Chou, J.-T. Hsu, *Proceedings the 11th Int'l. Congress on Advances in Non-Impact Printing Technologies*, IS&T, Springfield, VA, 1995, 125.
14. E. M. Williams, *The physics and technology of xerographic processes*, Wiley-Interscience, New York, 1984.
15. R. B. Lewis, E. W. Conners and R. F. Koehler, *4th Int'l. Conf. Electrophotogr.*, SPSE, Washington, D.C., 1981, paper no. 33.
16. C. N. Davies, *Aerosol Science*, Academic Press, London and New York, 1966.
17. W. R. Harper, *Contact and Frictional Electrification*, Oxford University Press, Oxford, 1967.
18. J. Lowell and A. C. Rose-Innes, *Adv. Physics*, **16**, 947 (1980).
19. J. T. Dickinson, E. E. Donaldson and M. K. Park, *J. Mater. Sci.* **16**, 2897 (1981).
20. J. T. Dickinson, L. C. Jensen and A. Jahan-Latibari, *J. Vac. Sci. Technol.* **A2**, 1112 (1984).
21. J. T. Dickinson and L. C. Jensen, *J. Polym. Sci.: Polym. Phys.* **23**, 873 (1985).
22. J. H. Anderson, *Proceedings of the 6th Int'l. Congress on Advances in Non-Impact Printing Technologies*, IS&T, Springfield, VA, 1990, 168, *J. Imaging Tech.* **16**, 204 (1994).
23. E. J. Gutman and G. C. Hartmann, *J. Imaging Sci. Technol.* **36**, 335 (1992).
24. E. J. Gutman and G. C. Hartmann, *J. Imaging Sci. Technol.* **39**, 285 (1995).